Coulomb blockade effect of molecularly suspended graphene nanoribbons investigated with scanning tunneling microscopy

Z. F. Zhong,[1] H. L. Shen,[2] R. X. Cao,[1] L. Sun,[1] K. P. Li,[1] J. Hu,[1] Z. Liu,[1] D. Wu,[1] X. R. Wang,[2,*] and H. F. Ding[1,†]

[1]*National Laboratory of Solid State Microstructures and Department of Physics, Nanjing University, 22 Hankou Road, Nanjing 210093, People's Republic of China*

[2]*National Laboratory of Solid State Microstructures and School of Electronic Science and Engineering, Nanjing University, 22 Hankou Road, Nanjing 210093, People's Republic of China*

(Received 20 June 2013; revised manuscript received 31 July 2013; published 4 September 2013)

We present the study of the quantum tunneling through a vertical two-barrier structure sandwiching a graphene nanoribbon quantum object. Scanning tunneling microscopy measurements of the graphene nanoribbon show staircase *I-U* characteristics and oscillating *dI*/*dU* spectra. To identify the physical origin of the observed effect, we varied the tunneling resistance of the tip-ribbon junction and found a tip-to-ribbon distance dependent oscillating period change. Together with the numerical analysis, we confirm that the resonances in the spectroscopy arise from the Coulomb blockade effect. The study of the Coulomb blockade effect in graphene nanoribbons may be of potential usages for the fabrication of superthin quantum dot devices.

DOI: 10.1103/PhysRevB.88.125408 PACS number(s): 73.23.Hk, 68.37.Ef, 72.80.Vp, 85.35.−p

I. INTRODUCTION

Graphene, a stable two-dimensional material with an atomically thin carbon layer, shows remarkable electronic and mechanical properties.[1–3] The outstanding electronic properties of graphene mainly arise from its marvelous linear band dispersion at low carrier energies so that its charge carriers travel like massless Dirac fermions.[4] In addition, graphene has excellent chemical and mechanical stability and can present ballistic transport property at room temperature.[5] These above features make graphene a promising candidate for post-silicon electronic devices.[6,7] In real applications like an electronic circuit, graphene often needs to be patterned into ribbons with nanometer in width, i.e., the graphene nanoribbons (GNRs). GNRs are quasi-1D graphene nanostructures with unique electronic properties that depend on their edge structures. Calculations based on tight binding predict that zigzag GNRs are always metallic while armchair GNRs can be either metallic or semiconducting, depending on their widths.[8–14] Localized states are found at the edge with energies close to the Fermi level in ribbons with zigzag edges. Moreover, a magnetic ordering is predicted and allowed to split the edge states, resulting in an antiferromagnetic coupling between two sides of the zigzag edges, which makes them a versatile material for new device design.[8,9,12,14] Recently, graphene and graphene nanoribbon based field effect transistors have attracted a lot of attention for their small size and high on/off switching ratio.[15–20] However, the metallic conductivity of graphene at the Dirac point impedes the use of graphene in electronic devices because field effect transistors made from graphene remain conducting even when the devices are switched off, which limits the achievable on/off switching ratio.[6,15,16,20–22] Field-effect tunneling transistors based on vertical graphene heterostructures have been developed and they are made of two graphene sheets sandwiched together with an atomically thin insulating barrier. These transistors increase the room-temperature switching ratios up to 10 000.[7] The tunneling of the electrons in the transistor from one graphene sheet to the other is similar to the single electron tunneling in Coulomb blockade phenomena. Coulomb blockade effects have been investigated in nanoscale tunnel junctions and junctions formed with a scanning tunneling microscope (STM) tip as one of the electrodes.[23–28] The effects have also been reported in planar graphene nanoribbon devices, which are induced by the chain of quantum dots due to localized edge states or bulk disorder in GNR.[29–32] The ultrahigh quality of GNR makes it possible to study the Coulomb blockade effects on GNRs, which may strengthen their potential usage in constructing new integrated microelectronic devices such as single electron memories and logic circuits.[33] Particularly, the use of GNR as part of the devices can dramatically reduce the size of the devices and may reduce the power consumption of electronic equipment greatly.

In this paper we present the study of the Coulomb blockade effect based on the quantum tunneling through a vertical two-barrier structure sandwiching a GNR quantum dot. The structure is formed by positioning a tip of STM on top of the GNRs suspended by small molecules on a Au(111) single crystal. STM measurements of the graphene nanoribbons show staircase *I-U* characteristics and pronounced oscillations in the *dI*/*dU* spectra. To identify the physical origin of the observed effect, we varied the tunneling resistance of the tip-GNR junction and found a tip-to-GNR distance dependent oscillating period change. Further numerical analysis confirms that the resonances in the spectroscopy of the GNR arise from the Coulomb blockade effect. Moreover, from the position dependent *dI*/*dU* spectra, we can derive that the GNR in our experiment forms a concave geometry with respect to the Au(111) surface, i.e., the edges of the GNR are higher than its middle. The study of the single electron tunneling observed in the vertical graphene two-barrier structure could be useful for the understanding of the mechanism of field-effect tunneling transistors based on vertical graphene heterostructures, and of potential usages for the fabrication of superthin quantum dot devices and single electron memories in the future.

II. EXPERIMENTAL TECHNIQUES

In our study, the nanoribbons are fabricated by unzipping pristine multiwall nanotubes (MWNTs) according to a method

that has been reported.[34–36] MWNTs are initially heated in air at 500 °C, which is a mild condition known to remove impurities and etch/oxidize MWNTs at defect sites and ends without oxidizing the pristine sidewall of the nanotubes. The nanotubes were then dispersed in a 1,2-dichloroethane (DCE) organic solution of poly(m-phenylenevinylene-co-2,5-dioctoxy-p-phenylenevinylene) (PmPV) by sonication, during which the nanotubes were found to be unzipped into nanoribbons. A Au(111) crystal was submerged into the freshly prepared solutions for ∼2 h to obtain a certain amount of GNR deposition. After an annealing process as previously reported, some of the GNRs are suspended by the remaining small molecules and the others have direct contact with the Au(111) surface.[37] STM imaging and spectroscopy measurements were performed at 4.8 K. The chemically etched W tips were *in situ* cleaned with an electron beam heating device to remove the W oxide at the tip end.[38] The bias voltage U refers to the sample voltage with respect to the tip. Spectroscopy measurements are performed via the modulation technique utilizing a 4-mV amplitude and 6.09-kHz frequency.

III. RESULTS AND DISCUSSION

Figure 1(a) presents a typical STM image of a GNR. It shows two parallel and straight edges with the width of about 20 nm. The scanning direction is from bottom to top. The gold surface is partially covered by small molecules remaining from the chemical treatment. These molecules sometimes cause the tip instability thus result in artifacts such as jumping lines as shown in Fig. 1(a) and its line profile in Fig. 1(b). The line profile across the nanoribbon, as marked by the blue line, shows the GNR is about 0.4 nm above the Au(111) surface, which evidences that the GNR is a single layer (the height of a single step in graphite is 0.34 nm).[14] The stronger contrasts at GNR edges suggest the edges are bended. The edges of the GNR seem to be ∼0.6 nm higher than the middle according to the STM image in Fig. 1(a) and its line profile in Fig. 1(b). STM is, however, not only sensitive to the morphology but also the electronic structures of GNR. Therefore, the line profile may also include information of the localized edge states and it is not straightforward to obtain the height information of the edges from STM topographic image only. As will be presented below, in combination with the position dependent dI/dU spectra, we can derive that the GNR in our experiment forms a concave geometry with respect to the Au(111) surface, i.e., the edges of the GNR are higher than its middle. A zoomed (atomic resolution) image Fig. 1(c) shows an almost perfect honeycomb structure, a hole surrounded by six carbon atoms. The imaging conditions are 1 V, 1 nA. The holes form a hexagonal pattern. Comparing the atomic resolution image with the edge direction, we learned that the GNR edge has an angle of 4.8 ° with respect to the zigzag direction, i.e., it is a (10, 1) ribbon as shown in Fig. 1(d).[37] The almost clean and defect-free surface suggests the GNRs are high-quality unzipping-derived GNRs, as previously reported.[14,36] Besides, the GNRs may have the self-cleaning and self-reknitting capability similar to as reported for graphene.[39] Good agreements are obtained by comparing the STM image with the lattice of the GNR with the zigzag edge as marked by the white grids. Some mismatches are also expected as the GNR surface is not perfectly flat due to the underlying small molecules.

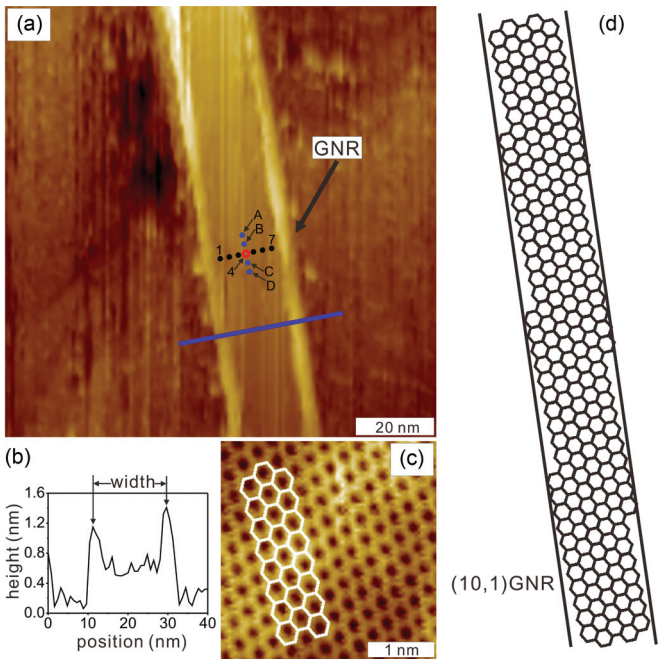

FIG. 1. (Color online) Typical STM images of a single layer GNR. (a) Morphology of GNR on Au(111). (b) Line profile across the GNR as marked by the blue line in (a). (c) Atomic resolved image of the same GNR in (a). The white honeycombs are lattice of GNR with a zigzag edge. The imaging conditions are 1 V, 1 nA. (d) Structure model of a (10,1) GNR.

Figure 2(a) shows the typical I-U curve taken in the nanoribbon at the position marked by the red circle in Fig. 1(a). We can find that a good staircaselike characteristic presented at the bias ranged from -0.6 to -0.3 V. The effects are more pronounced in the simultaneously taken bias-voltage dependent dI/dU curve [black curve in Fig. 2(b)]. The peaks in the dI/dU curve on the GNR had equidistant spacing of 91.2 meV. The tip is stabilized at 0.6 V, 1 nA during the spectroscopy measurements. To exclude the tip induced effect, we also performed similar measurements about 50 nm away from the GNR. We note that in between no apparent tip change occurred as the following spectrum takes on the GNR remain unchanged. We can find that the profound oscillations are only present in the dI/dU spectrum on the GNR, while the spectrum on the molecular coated Au surface does not show such characteristics. Therefore, we can exclude the strange tip effect. We also performed similar measurements at the locations both perpendicular to and parallel to the edge of the GNR as marked by the red circle (center position, i.e., position 4), the black dots (positions 1–3 and 5–7 from left to right), and the blue dots (position A–D) in Fig. 1(a). The results are plotted in Fig. 2(c). We can find that the oscillation period varied when the STM tip moved perpendicular to the ribbon direction. The oscillation period measured on the middle of the GNR is larger than that measured near the two sides of the GNR. On the contrary, less variation was obtained when the tip moved parallel to the ribbon. The small variations of the oscillation period along the GNR edge could

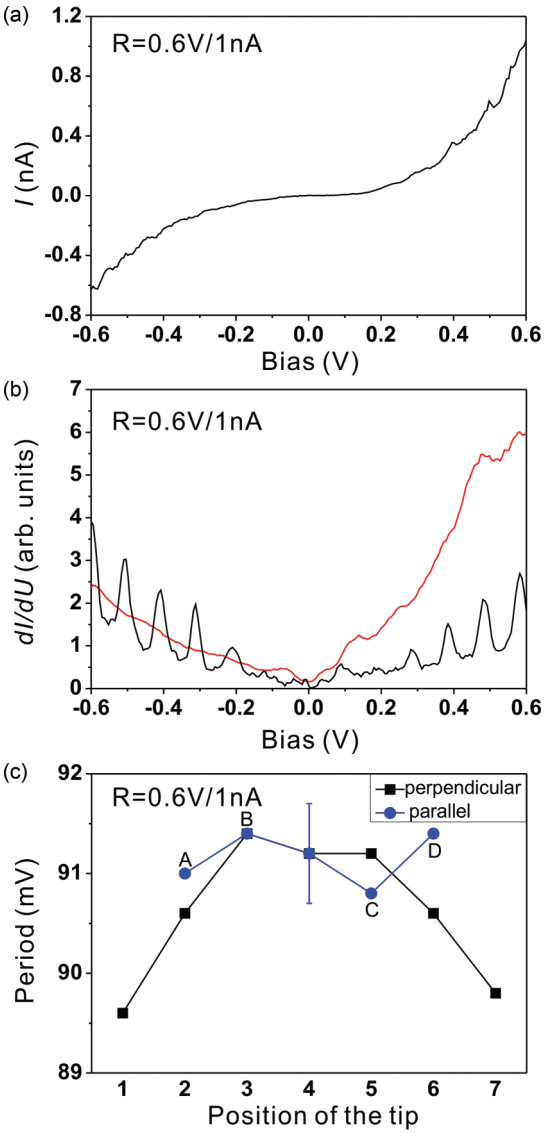

FIG. 2. (Color online) (a) A typical I-U curve taken in the graphene nanoribbon at the position marked by the red circle in Fig. 1(a). (b) The black curve is a typical bias dependent dI/dU curve simultaneously taken at the same position as in (a). The red curve is a dI/dU curve taken on the molecular coated Au surface which is about 50 nm away from the GNR. (c) The oscillation periods of the spectroscopy measured in the direction perpendicular to and parallel to the nanoribbon edge at the position marked by the red circle, and the black/blue dots in Fig. 1(a). The tunneling resistance R is 0.6 V/1 nA in (a), (b), and (c).

be associated with the random distribution of the molecules under the GNR. The oscillations in the spectroscopy could be associated with the quantum confinement in the direction perpendicular to the edge, the quantum Hall effect[40–44] or the Coulomb blockade effect.[23,25,27,28,30] Previous measurement of GNR, however, did not show any clear oscillation in the spectroscopy of GNR.[14] Moreover, if the oscillation is caused by the quantum confinement effect, one would expect it would be a constant, independent with the tip positioning. This is in sharp contrast with the experimental observation in Fig. 2(c). Therefore, we could exclude the quantum confinement effect

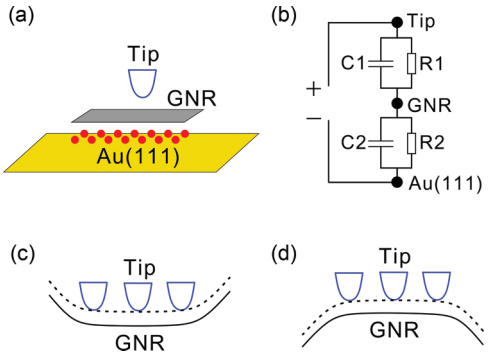

FIG. 3. (Color online) (a) Schematic drawing of the two-tunnel junction configuration in our experiment. One tunnel junction with variable electrode separation is formed between the STM tip and the GNR, and a second fixed tunnel junction is formed between the GNR and the Au(111). The red balls represent the small molecules remained from the chemical treatment. (b) Equivalent circuit for this system where R_1 and R_2 are the tunneling resistances of the tip-GNR and the GNR-Au(111) junctions, and C_1 and C_2 are the capacitances of these junctions, respectively. (c) and (d) The schematic drawing of STM tips on a concave GNR and a convex GNR at different positions. The dashed lines show the trace of the tip-end of STM in a constant current mode scan.

from the origin of the observed effect. The quantum Hall effect usually requires the presence of magnetic field or strain in the system.[40,41] In our measurements, no magnetic field was applied. The atomic resolution image also showed no apparent strain in the GNR. Therefore, the observed oscillations in the spectroscopy cannot be the magnetic field or strain induced quantum Hall effect either.

Therefore, we attribute the observed regular oscillations to the Coulomb blockade. The Coulomb blockade effect can be described as the quantum mechanical tunneling of electrons through a quantum dot with two weakly coupled leads. Figure 3(a) shows the schematic model in our experiment. The two-barrier tunnel junction is formed by positioning a STM tip on top of a GNR, which is suspended by small molecules on a Au(111) surface. The three conductive elements, i.e., the STM tip, the GNR, and the Au(111), are isolated from each other by vacuum or the insulating molecules as marked. The small molecules are likely the surfactant from the chemical unzipping process. Figure 3(b) shows the equivalent circuit for this system where R_1 and R_2 are the tunneling resistances of the tip-GNR and the GNR-Au(111) junctions, and C_1 and C_2 are their capacitances, respectively. In such junctions, the transfer of a single electron between the junction electrodes increases the electrostatic energy by $\Delta E = e^2/C$, where $C = 1/(\frac{1}{C_1} + \frac{1}{C_2})$ is the junction capacitance.[26,27] When the thermal energy $k_BT \ll e^2/C$, this energy is unavailable at small voltage biases, and the electron tunneling is suppressed.[23–25] In such cases, the electrical transport is hindered until a new potential match is reached. Therefore, the transport is quantized, leading to a ladder-shape I-U curve and pronounced oscillations in the dI/dU spectrum. The oscillation period is inversely proportional to the total capacitor of the junction. If one of the capacitors is changed, the oscillation period should also be varied accordingly. On the other hand, if the oscillation is caused by the other two mechanisms discussed above, the

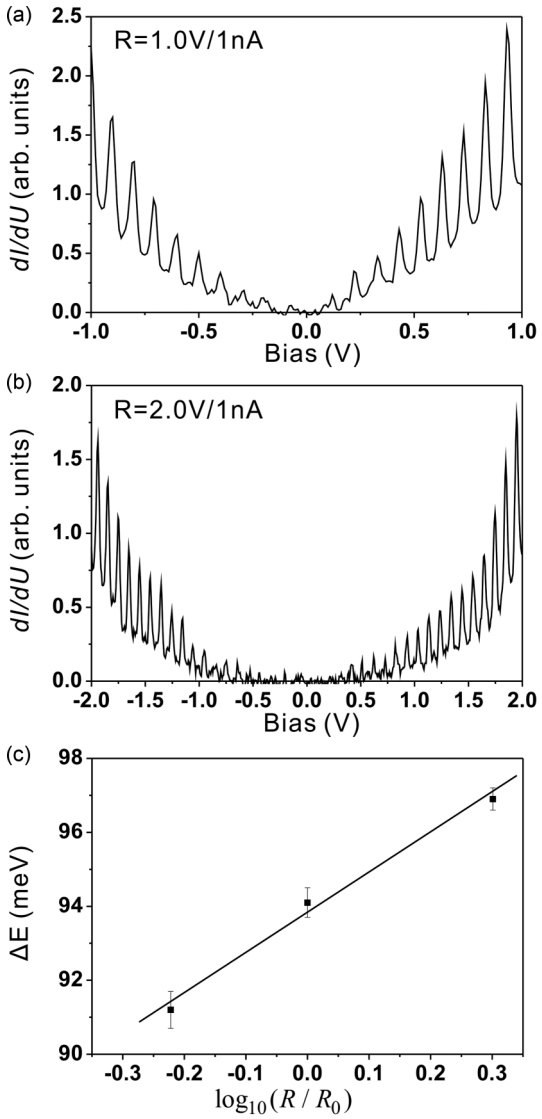

FIG. 4. (a) and (b) Typical bias dependent *dI*/*dU* curves taken in the nanoribbon at the position marked by the red circle in Fig. 1(a). The tunneling resistance R is 1.0 V/1 nA in (a) and 2.0 V/1 nA in (b), respectively. (c) The relationship between the spacing of the oscillation peaks and the tunneling resistance R.

period should be independent with the tip-sample distance. This provides a method to distinguish the Coulomb blockade effect from the other mechanisms. In this particular geometry, the capacitor can be tuned by modifying the tip-sample separation d since $C_1 = \frac{\varepsilon_0 S}{d}$ by assuming that the capacitor is formed by two parallel plates. ε_0 is the permittivity of the vacuum, and S is the effective area of the parallel plates.

Therefore, we performed similar measurements but with different tunneling resistance. When the tunneling resistance changes, the distance between the tip and the GNR is also changed, resulting in a change of the capacitance between them. Figures 4(a) and 4(b) show the *dI*/*dU*-*U* curves obtained at the same position of the GNR, as marked by the red circle in Fig. 1(a). The tunneling resistance is 1.0 and 2.0 V/1 nA in Figs. 4(a) and 4(b), respectively. We find that the oscillation period among the peaks in the spectra changes to 94.1 and 96.9 meV in Figs. 4(a) and 4(b), respectively. The change of the oscillation period with the tip-GNR separation strongly suggests that the observed phenomena are the Coulomb blockade effects. In addition, the observed increase of the oscillation period with the increasing tip-GNR separation is also in qualitative agreement with the theory of Coulomb blockade effect as $\Delta E = e^2/C$ and that the capacitance is inversely proportional to the separation between two electrodes.[26,27]

To make a quantitative comparison, we plot the oscillation period as a function of the tunneling resistance with logarithmic coordinates in Fig. 4(c). As discussed above, the oscillation period $\Delta E = \frac{e^2}{C} = e^2(\frac{1}{C_1} + \frac{1}{C_2})$ in Coulomb blockade effect. In our measurements, C_2 is assumed to be a constant as the separation between GNR and gold surface is fixed. One can simplify the tip-GNR capacitance C_1 as a capacitor of the two parallel plates and estimate the capacitance to be $C_1 = \frac{\varepsilon_0 S}{d}$. Typically, the tunneling resistance varies about one order per 0.1 nm and the tip-sample separation in STM can be described as $d \approx d_0 + \log_{10}(R/R_0) \times 0.1$ in the unit of nm.[45,46] R is the tip-GNR tunneling resistance and d_0 is the tip-sample separation when the tunneling resistance $R_0 = 1$ V/1 nA $= 10^9$ Ω. Therefore, we can obtain the relationship between the spacing of the oscillation peaks ΔE and the tunneling resistance R that $\Delta E \approx e^2[\frac{d_0+\log_{10}(R/R_0)\times 0.1}{\varepsilon_0 S} + \frac{1}{C_2}]$. And a linear dependence of ΔE versus $\log_{10}(R/R_0)$ is expected. The experimental results plotted in Fig. 4(c), indeed, show a clear linear dependence. This, together with the *I*-*U* steps and the equidistant spacing oscillation in the *dI*/*dU*-*U* curve incontrovertibly confirms that the observed phenomena are the single electron tunneling. According to the slope of the line plotted in Fig. 4(c), we can obtain the effective area of the parallel plates to be 170 nm^2. In our experiments we used electrochemical etched W tips. Typically tips with a sharpness of 5–50 nm are obtained depending on the etching condition. The experimental probed GNR has the width of 20 nm. From this we can also estimate an effective area to be in the order of 20–200 nm^2, in good agreement with the above estimation. Following Dürig *et al.* and assuming the STM tip end is a paraboloid, we can estimate the gap width between the tip and the GNR to be about 0.5 nm when the tunneling conductance is $G = 1$ nA/1 V $= 10^{-9}$ Ω^{-1}.[47] With that we obtained $C_1 = \frac{\varepsilon_0 S}{d_0} = 3.19 \times 10^{-18}$F and $C_2 = 3.64 \times 10^{-18}$F when the tunneling resistance is 1.0 V/1 nA. As both the accurate separation between the GNR and the Au(111) surface and the permittivity of the molecules are unknown, it is difficult to obtain the effective area of the second capacitance C_2. We expected it is similar to that of the first capacitance, i.e., around 170 nm^2.

The starting peak of the oscillation in the spectrum appears at about 0.1 V at the resistance of 0.6 and 1.0 V/1 nA as shown in Figs. 2(b) and 4(a), while the first peak in Fig. 4(b) seems to be close to 0.5 V, which is almost five times larger than in Figs. 2(b) and 4(a). At 2.0 V/1 nA, the magnitude of the starting peak is too small to distinguish itself from the noise level due to the small tunneling current at small bias. In our oscillation period analysis, only the sharp and distinct peaks in the *dI*/*dU* spectrum are taken into account in order to obtain a reliable conclusion. From Fig. 1(d) we can find that the (10,1) nanoribbon is close to the zigzag-edge GNR.

In Ref. 14, a gap of about 25 meV is opened at the edge of the GNR near the Fermi level for a (8,1) nanoribbon of 15 nm wide. But the spectrum probed 2.5 nm away from the edge on the flat GNR shows no distinct characteristics or any gap. As the gap decays from the edge to the center, it is attributed to be originated from the electron-electron interaction between the two edges of the GNR. This is also supported by the band structure calculations. We would expect a (10,1) GNR behaves similar as a (8,1) GNR as their edge structures are quite similar. Only the gap is smaller as it has a width of 20 nm which is wider than that of a (8,1) GNR. Following their analysis, we estimate the gap to be 20 meV and it should decay from the edge to the center part of the GNR, similar to the observation on a (8,1) GNR. Our measurements were performed near the center position of the GNR. In such a case, no gap is expected in good agreement with our experimental findings.

In our experiment, the GNRs are deposited on Au(111) from the PmPV solution. When the GNRs are loaded, the GNRs may form the concave or convex geometries with respect to the Au(111) surface. As we present in Fig. 1(b), the line profile of the GNR implies that the GNR could be a concave GNR. Since GNRs have the edge states, the line profile of the GNR may also include the information of the localized edge states. Therefore, it is hard to identify whether the GNRs form the concave or convex geometry from the STM morphology image only. The position dependent Coulomb blockade measurements may provide additional information to distinguish these two configurations. Figures 3(c) and 3(d) show the schematic drawing of STM tips on a concave GNR and a convex GNR at different positions. The dashed line shows the trace of the tip-end in constant current mode scan. From the model shown in Fig. 3(c), we can find that S, the effective area of the capacitor formed by the tip and the GNR, will increase when the tip moves from the middle to the side for a concave GNR. This will cause the oscillation period ΔE to decrease according to $C_1 = \frac{\varepsilon_0 S}{d}$ and $\Delta E = \frac{e^2}{C} = e^2(\frac{1}{C_1} + \frac{1}{C_2})$. On the contrary, the change will be the opposite for a GNR in convex configuration with the Au(111). In our experiment, we find that the oscillation period observed in the spectroscopy decreases when the tip moves from the middle to the side as shown in the black curve of Fig. 2(c). Therefore, we could conclude that the GNR we observed in our experiment is a concave GNR, i.e., the edges of the GNR are higher than its middle. Quantitatively, the oscillation period decreases 2 meV, i.e., from ∼91 meV at the GNR center to ∼89 meV at the location about 4 nm away from the center (position 1 and 7). Assuming this change is purely originated from increase of the effective area, it is about 2.2%. We can also estimate the area change by assuming the STM tip has an end with the shape of 5 nm radius hemisphere. From the line profile shown in Fig. 1(b), the GNR has a flat area with the width of 14 nm in the center region. Assuming a linear bending at the GNR edge, we obtained about 3% effective area change from center to positions 1 and 7, in good agreement with the experimental finding. In addition, the increasing separation between the GNR and the Au(111) surface at the GNR edge may also influence the oscillation period change as it will change C_2. This influence, however, is not significant since the separation increase is about 0.5 nm at the edge, which is much smaller than the estimated separation of several nm. The weak variations (∼0.5 mV) of the oscillation period in the dI/dU spectrum along the GNR as shown in Fig. 2(c) could be attributed to the disordered molecular layer randomly covering the Au(111) surface. As the effective area is about 170 nm^2, the fluctuation caused by the random distribution of small molecules is averaged and turns out to be small. The variation is smaller than the oscillation period change perpendicular to the GNR [black curve in Fig. 2(c)] and the change measured in Fig. 4(c), which is about 6 mV. This excludes the noise as the origin of the observed effects.

IV. SUMMARY

In summary, utilizing scanning tunneling microscopy, we observed the ladder shape I-U curve and equidistant spacing oscillations in the dI/dU-U curve on the graphene nanoribbon suspended by small molecules on Au(111). By changing the tunneling conditions, we found a linear dependence of the oscillation period versus the tip-to-sample distance. This evidences that the observed effect is the Coulomb blockade effect. Moreover, the position dependent measurements across the GNR can provide additional information to identify whether the GNR form a concave or convex geometry with the Au(111) surface. The study of the single electron tunneling in the vertical graphene two-barrier structure could be helpful for the understanding of the mechanism of field-effect tunneling transistors based on vertical graphene heterostructures and of potential usages for the fabrication of superthin single electron memories and quantum dot devices.

ACKNOWLEDGMENTS

This work is supported by the State Key Program for Basic Research of China (Grants No. 2010CB923401 and No. 2013CBA01600), NSFC (Grants No. 11374145, No. 11023002, and No. 11274154), and NSF of Jiangsu (Grant No. BK2012300).

*Corresponding author: xrwang@nju.edu.cn
†Corresponding author: hfding@nju.edu.cn

[1] K. S. Novoselov, A. K. Geim, S. V. Morozov, D. Jiang, M. I. Katsnelson, I. V. Grigorieva, S. V. Dubonos, and A. A. Firsov, Nature (London) **438**, 197 (2005).
[2] S. Stankovich, D. A. Dikin, G. H. B. Dommett, K. M. Kohlhaas, E. J. Zimney, E. A. Stach, R. D. Piner, S. T. Nguyen, and R. S. Ruoff, Nature (London) **442**, 282 (2006).
[3] S. Ghosh, D. L. Nika, E. P. Pokatilov, and A. A. Balandin, New J. Phys. **11**, 095012 (2009).

[4] A. H. Castro Neto, F. Guinea, N. M. R. Peres, K. S. Novoselov, and A. K. Geim, Rev. Mod. Phys. **81**, 109 (2009).
[5] A. K. Geim and K. S. Novoselov, Nat. Mater. **6**, 183 (2007).
[6] A. K. Geim, Science **324**, 1530 (2009).
[7] L. Britnell, R. V. Gorbachev, R. Jalil, B. D. Belle, F. Schedin, A. Mishchenko, T. Georgiou, M. I. Katsnelson, L. Eaves, S. V. Morozov, N. M. R. Peres, J. Leist, A. K. Geim, K. S. Novoselov, and L. A. Ponomarenko, Science **335**, 947 (2012).
[8] K. Nakada, M. Fujita, G. Dresselhaus, and M. S. Dresselhaus, Phys. Rev. B **54**, 17954 (1996).
[9] H. Lee, Y.-W. Son, N. Park, S. Han, and J. Yu, Phys. Rev. B **72**, 174431 (2005).
[10] M. Ezawa, Phys. Rev. B **73**, 045432 (2006).
[11] Y. W. Son, M. L. Cohen, and S. G. Louie, Nature (London) **444**, 347 (2006).
[12] Y.-W. Son, M. L. Cohen, and S. G. Louie, Phys. Rev. Lett. **97**, 216803 (2006).
[13] H. Zheng, Z. F. Wang, T. Luo, Q. W. Shi, and J. Chen, Phys. Rev. B **75**, 165414 (2007).
[14] C. Tao, L. Jiao, O. V. Yazyev, Y.-C. Chen, J. Feng, X. Zhang, R. B. Capaz, J. M. Tour, A. Zettl, S. G. Louie, H. Dai, and M. F. Crommie, Nat. Phys. **7**, 616 (2011).
[15] F. Schwierz, Nature (London) **472**, 41 (2011).
[16] S.-J. Han, K. A. Jenkins, A. Valdes Garcia, A. D. Franklin, A. A. Bol, and W. Haensch, Nano Lett. **11**, 3690 (2011).
[17] X. Li, X. Wang, L. Zhang, S. Lee, and H. Dai, Science **319**, 1229 (2008).
[18] Y. Ouyang, X. Wang, H. Dai, and J. Guo, Appl. Phys. Lett. **92**, 243124 (2008).
[19] X. Wang, Y. Ouyang, X. Li, H. Wang, J. Guo, and H. Dai, Phys. Rev. Lett. **100**, 206803 (2008).
[20] L. Liao, Y.-C. Lin, M. Bao, R. Cheng, J. Bai, Y. Liu, Y. Qu, K. L. Wang, Y. Huang, and X. Duan, Nature (London) **467**, 305 (2010).
[21] F. Schwierz, Nat. Nanotech. **5**, 487 (2010).
[22] Y.-M. Lin, A. Valdes-Garcia, S.-J. Han, D. B. Farmer, I. Meric, Y. Sun, Y. Wu, C. Dimitrakopoulos, A. Grill, P. Avouris, and K. A. Jenkins, Science **332**, 1294 (2011).
[23] P. J. M. van Bentum, R. T. M. Smokers, and H. van Kempen, Phys. Rev. Lett. **60**, 2543 (1988).
[24] M. Amman, R. Wilkins, E. Ben-Jacob, P. D. Maker, and R. C. Jaklevic, Phys. Rev. B **43**, 1146 (1991).
[25] A. E. Hanna and M. Tinkham, Phys. Rev. B **44**, 5919 (1991).
[26] M. Amman, S. B. Field, and R. C. Jaklevic, Phys. Rev. B **48**, 12104 (1993).
[27] W. Chen, H. Ahmed, and K. Nakazoto, Appl. Phys. Lett. **66**, 3383 (1995).
[28] H. Imamura, J. Chiba, S. Mitani, K. Takanashi, S. Takahashi, S. Maekawa, and H. Fujimori, Phys. Rev. B **61**, 46 (2000).
[29] F. Sols, F. Guinea, and A. H. Castro Neto, Phys. Rev. Lett. **99**, 166803 (2007).
[30] S. Dröscher, H. Knowles, Y. Meir, K. Ensslin, and T. Ihn, Phys. Rev. B **84**, 073405 (2011).
[31] D.-K. Ki and A. F. Morpurgo, Phys. Rev. Lett. **108**, 266601 (2012).
[32] X. Wang, Y. Ouyang, L. Jiao, H. Wang, L. Xie, J. Wu, J. Guo, and H. Dai, Nat. Nanotech. **6**, 563 (2011).
[33] K. Nakazato and H. Ahmed, Adv. Mater. **5**, 668 (1993).
[34] L. Jiao, L. Zhang, X. Wang, G. Diankov, and H. Dai, Nature (London) **458**, 877 (2009).
[35] L. Xie, H. Wang, C. Jin, X. Wang, L. Jiao, K. Suenaga, and H. Dai, J. Am. Chem. Soc. **133**, 10394 (2011).
[36] L. Jiao, X. Wang, G. Diankov, H. Wang, and H. Dai, Nat. Nanotech. **5**, 321 (2010).
[37] Z. F. Zhong, H. L. Shen, R. X. Cao, L. Sun, K. P. Li, X. R. Wang, and H. F. Ding, J. Appl. Phys. **113**, 174307 (2013).
[38] H. F. Ding, J. E. Pearson, D. Li, R. Cheng, F. Y. Fradin, and S. D. Bader, Rev. Sci. Instrum. **76**, 123703 (2005).
[39] R. Zan, Q. M. Ramasse, U. Bangert, and K. S. Novoselov, Nano Lett. **12**, 3936 (2012).
[40] Y. Zhang, Y.-W. Tan, H. L. Stormer, and P. Kim, Nature (London) **438**, 201 (2005).
[41] K. S. Novoselov, E. McCann, S. V. Morozov, V. I. Fal'ko, M. I. Katsnelson, U. Zeitler, D. Jiang, F. Schedin, and A. K. Geim, Nat. Phys. **2**, 177 (2006).
[42] E. McCann and V. I. Fal'ko, Phys. Rev. Lett. **96**, 086805 (2006).
[43] N. Levy, S. A. Burke, K. L. Meaker, M. Panlasigui, A. Zettl, F. Guinea, A. H. Castro Neto, and M. F. Crommie, Science **329**, 544 (2010).
[44] F. Guinea, M. I. Katsnelson, and A. K. Geim, Nat. Phys. **6**, 30 (2010).
[45] G. Binnig, H. Rohrer, C. Gerber, and E. Weibel, Appl. Phys. Lett. **40**, 178 (1982).
[46] G. Binnig and H. Rohrer, IBM J. Res. Dev. **44**, 279 (2000).
[47] U. Dürig, O. Züger, and D. W. Pohl, J. Microsc. **152**, 259 (1988).